Z. Phys. A 350, 215–219 (1994)

ZEITSCHRIFT
FÜR PHYSIK A

Spin alignment of ^{43}Sc produced in the fragmentation of 500 MeV/u ^{46}Ti

W.-D. Schmidt-Ott[1], K. Asahi[2], Y. Fujita[3], H. Geissel[4], K.-D. Gross[4], T. Hild[1], H. Irnich[5], M. Ishihara[6], K. Krumbholz[1], V. Kunze[1], A. Magel[5], F. Meissner[1], K. Muto[2], F. Nickel[4], H. Okuno[7], M. Pfützner[4], C. Scheidenberger[4], K. Suzuki[7], M. Weber[4], C. Wennemann[1]

[1] II. Physikalisches Institut der Universität, D-37073 Göttingen, Germany
[2] Faculty of Science, Tokyo Institute of Technology, Megro-ku, Tokyo 152, Japan
[3] Department of Physics, Osaka University, Toyonaka, Osaka 560, Japan
[4] GSI, Postfach 110552, D-64220 Darmstadt, Germany
[5] II. Physikalisches Institut der Universität, D-35392 Giessen, Germany
[6] Department of Physics, The University of Tokyo, Bunkyo-ku, Tokyo 113, Japan
[7] Institute of Physical and Chemical Research (RIKEN), Wako-shi, Saitama 351-01, Japan

Received: 25 July 1994

Abstract. In the fragmentation of 500 MeV/u ^{46}Ti the spin alignment of ^{43m}Sc ($I=19/2^-$, $T_{1/2}=473$ ns) fragments was observed by the Time Dependent Perturbed Angular Distribution (TDPAD) method. The measurement was performed for different cuts in the longitudinal momentum distribution. A positive spin alignment of about 35% was observed in the center and a negative alignment of about 15% in the wing of the distribution. For the different cuts the relative production of the $19/2^-$ state was measured. In the wing of the distribution the isomeric ratio N($19/2^-$)/total ^{43}Sc is about 15 times larger than in the center. The results of this pilot experiment are discussed in the frame of a shell-model.

PACS: 25.70.Np; 23.20.En; 21.60.−n

1. Introduction

The effect of spin polarization in nuclear reactions is well known. At low projectile energies the polarization is explained by friction-like forces for close trajectories [1]. A different process is considered at higher projectile energies. In peripheral encounters between projectile and target one or more nucleons are removed from the projectile and the motion of the removed cluster is reflected in the angular momentum distribution of the fragment [2].

At Fermi energies we have observed an alignment in a 0°-experiment [3]. However, from a theoretical standpoint [4], it was expected that the underlying model calculations would fit better to much higher projectile energies. A lower limit of 500 MeV/u was proposed [4].

We here report on a first experiment at such energies where we found indication for a large alignment. Thus, the present and further measurements can be an important clue for the understanding of the high-energy fragmentation process.

2. Experimental method

We used a projectile beam of 500 MeV/u ^{46}Ti from the SIS accelerator facility at GSI Darmstadt [5]. The beam intensity was of the order of 10^9 particles per 2s-spill, directed in a slow extraction mode onto a 1006 mg/cm^2 beryllium target mounted at the entrance of the fragment separator FRS. The ^{43}Sc nuclei were separated from other fragments and from the primary beam by A/Z and energy-loss selection. The target introduced a spread of less than 10% of the total longitudinal momentum width of the Goldhaber distribution [6, 7]. The intensity of the secondary ^{43}Sc beam reached $\sim 10^4$ particles per spill. Cuts in the longitudinal momentum distribution were selected and typical implantation rates of 10^3 ions per spill were measured with the silicon detector $E2$ in front of a stopper at the final focus (see Fig. 1).

A position-sensitive scintillator in the middle plane of the fragment separator FRS was used to measure the spatial distribution of the ^{43}Sc fragments from the reaction. The ^{43}Sc nuclei were selected in the analysis by gates on the fragments detected in the silicon counter $E2$, and on the scandium ($Z=21$) peak in the MUSIC energy-loss spectrum (see inset of Fig. 1). The spatial width of 70(3) mm can be converted into a total-momentum width of 0.75% in the rest system of the fragment [6]. In order to cut selected bins from this momentum distribution, the $S1$ slit [8] was operated. With the selected momentum bins, the FRS was tuned to refocus the ^{43}Sc fragments into the stopper. One of the resulting momentum spectra of ^{43}Sc is given in Fig. 2.

A purity of 79(4)% ^{43}Sc of the implanted nuclei was measured using the total momentum distribution by two independent methods. First, we measured the two-dimensional plot of the energy-losses in the silicon detectors $E1$ and $E2$ placed at the final focus and compared the region of ^{43}Sc with the total number of arriving ions. Second, the number of ^{43}Sc ground-state decays ($T_{1/2}=3.9$ h) was measured subsequent to a several-hour-implantation and compared with the total number of implanted ions during this period.

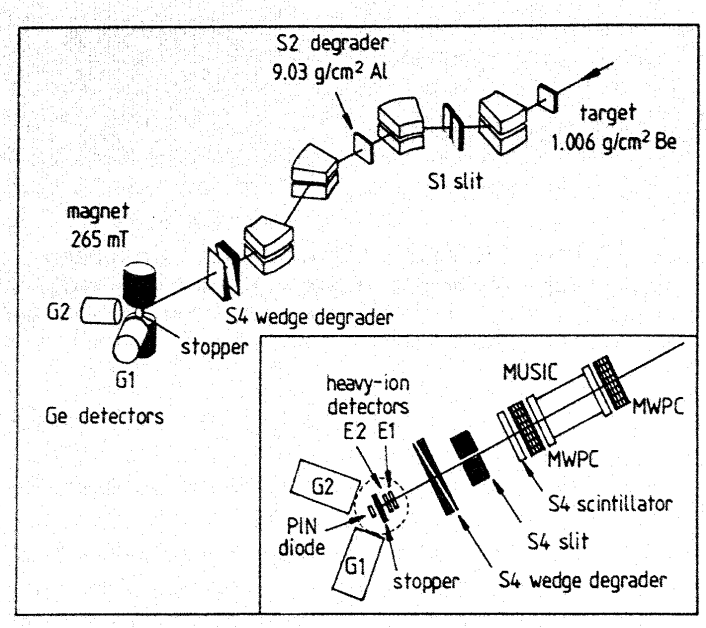

Fig. 1. Experimental set-up at the fragment separator FRS. Inset: the region of fragment implantation at the final focus *S4*

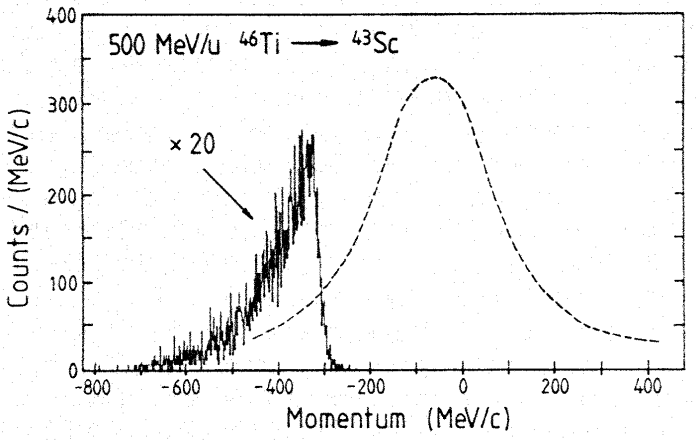

Fig. 2. Experimental momentum distribution of ^{43}Sc after fragmentation of 500 MeV/u ^{46}Ti projectiles, achieved by cutting the total distribution (*dashed curve*) with a slit at the *S1* focal plane (*see Fig. 1*)

The thickness of the *S4* degrader was adjusted for the correct implantation of fragments. The range profiles were measured as a function of the degrader thickness using the silicon detectors *E1* and *E2* and a veto PIN diode behind the stopper (see inset of Fig. 1). For reference, the count rate of a scintillator at *S4* was taken.

In order to perform TDPAD measurements, we made the following set-up. The stopper was mounted in a perpendicular magnetic field of 0.265 *T* with a homogenity of ~1% at the implantation area. The field polarity was changed as a parameter during the run. Three metallic stoppers of 3 mm thick Al, 2.6 mm thick In, and 1.9 mm thick Pb were used to test which material was optimal for the conservation of the spin alignment. The stoppers had a diameter of 30 mm and could be remotely exchanged during the experiment.

Outside the magnet with its 38 mm gap, two Ge-detectors with a standard efficiency of 70% were placed in a distance of 6 cm to the stopper. In order to measure the angular distribution of the γ-cascades, the detectors were set at $+45°$ and $-45°$ with respect to the incoming beam. The length (91 mm) and the diameter (70 mm) of the crystals may be compared with a $3'' \times 3''$ NaI crystal for estimation of the finite solid angle correction (see below).

The measured time-to-amplitude converter (TAC) spectra were started by the arrival of a ^{43}Sc ion in the detector *E2* and stopped by the γ-decays. In the decay of the $I = 19/2^-$ isomer, the cascading γ-rays of 136, 1158, and 1830 keV were measured. We also measured 152 keV γ-radiation of the $3/2^+$ isomer ($T_{1/2} = 0.44$ ms). The counting was done during the 2*s*-beam-on spill for 4 μs-periods after each *E2* start signal. In this 4 μs-window the exponential decay of the $19/2^-$ isomer with a half-life of 473 ns was well observed while only a small part of the $3/2^+$ isomer was detected.

3. Experimental results

3.1. Spin alignment

The TAC spectra started by the arrival of a ^{43}Sc fragment in *E2* and stopped by the γ-decay of the $19/2^-$ isomer were measured with the two Ge detectors giving the experimental count rates $N1(t)$ and $N2(t)$. We selected the events of the γ-lines at 1158 and 1830 keV. The function $R(t) = (N1 - N2)/(N1 + N2)$ eliminates the exponential decay and is the basis for the TDPAD method [9]. The $R(t)$ data derived from the experimental $N1(t)$ and $N2(t)$ TAC spectra are shown in Fig. 3 for two selected runs.

The universal routine MINUIT [11] was used to fit a harmonic oscillation, $R(t) = r \cdot \sin\{2\pi(t - T_0)/T_{osc}\} + c$,

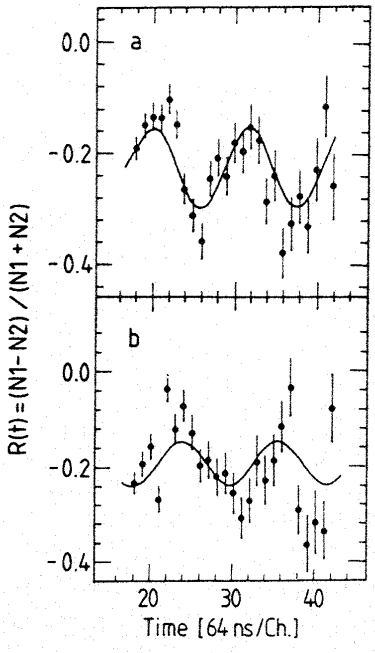

Fig. 3. Experimental values $R(t)$ measured with a Pb stopper in a magnetic field of **a** -0.265 T and **b** 0.265 T. The *line* shows the MINUIT [11] fit with a fixed period of 750 ns. For details, *see text*

to the data excluding the prompt coincidence peak. The fit parameters are the amplitude r, the ordinate off-set c, a phase shift given by T_0 and a fixed value of T_{osc}. In a first attempt all four parameters were fitted. It was found, however, that the results for the oscillation period T_{osc} corresponded very well to the expected period of 750 ns. Therefore, in the rest of the analysis, T_{osc} was fixed at 750 ns. An off-set c can be explained by different efficiencies of the γ-detectors, provided that the fragments were not stopped in the center of the implantation target. In fact, the observed shifts in the ordinate correspond to beam displacements of about 1 cm in the horizontal plane.

As can be seen from Figs. 3a and b, a phase shift of the fitted $R(t)$ functions was found when changing the direction of the magnetic field. A similar phase shift was observed for the same field direction when comparing the data for the momentum bins in the center and in the wing of the Goldhaber distribution. The results from the fit procedure indicate that in both cases the phase shift could be somewhat smaller than the expected value π.

For the stopper materials In and Pb, no significant difference in amplitude r of the $R(t)$ function was observed for otherwise identical parameters. The smallest amplitude was measured for Al stoppers.

3.2. Isomeric ratios

Within the 4 μs time-interval after the detection of the ^{43}Sc ions, the γ-decay of the $19/2^-$ isomer ($T_{1/2}=473$ ns) was measured. The decay of the $3/2^+$ isomer ($T_{1/2}=0.44$ ms) was measured in the 2s beam-on intervals. During the time-of-flight through the separator, 50% of the produced $19/2^-$ isomers had decayed before implantation. For the completely stripped ions a half-life increase of $\sim 10\%$ caused by the missing internal conversion was taken into account. The production ratios of the two isomers for the different momentum bins were obtained from γ-ray intensity ratios, corrected for the γ-ray efficiencies of the respective radiation. The measurement of the isomeric ratio $(19/2^-)$/total ^{43}Sc includes the counting of the implanted ^{43}Sc fragments (see above). For the selected momentum cuts the resulting production ratios are summarized in Table 1.

4. Discussion

In the fragmentation of 500 MeV/u ^{46}Ti, the formation of $19/2^-$ and $3/2^+$ isomeric states in ^{43}Sc was observed and the alignment of the $19/2^-$ isomer was measured. The alignment introduced by the fragmentation reaction survived the deceleration of the fragments with an incoming velocity of $\sim 0.7 \cdot c$ along the 74 m flight-path in the FRS spectrometer. Before implanting the fragments, the last degrading was performed in the $S4$ degrader. Finally, the ions passed 50 cm air with energies of ~ 50, ~ 80, and ~ 95 MeV/u for the Al, In, and Pb stopper. At these energies, the electron capture cross-sections of the fully-stripped ions are not negligible.

Table 1. Production of the ^{43}Sc isomers for different momentum cuts

Momentum cut	$19/2^-$/total ^{43}Sc (%)	$19/2^-/3/2^+$ (%)
Center	0.74(7)	2.2(1)
Intermediate	3.2(3)	12.1(6)
Wing (Fig. 2)	11.9(11)	24(1)

The dealignment by hyperfine interaction during the flight was estimated from [12] and gave a small correction for the alignment measured with In and Pb stoppers, where in the case of the Al stopper the dealignment may exceed 20%.

According to a recent measurement with ^{43m}Sc ($I=19/2^-$) implanted with low energies, no different behaviour in the three stopper materials was observed [13]. In fact, the interaction of the spins with the stopper-lattice (which would destroy the alginment) is small and has a relaxation time of the order of milliseconds [14].

In order to explain the observed oscillation of the $R(t)$ function (see above) the theory of angular distribution of γ-rays emitted from oriented states [9] is applied. The following expression holds for this correlation:

$$W(\vartheta)=\sum_{k=0,2,4} Q_k \cdot \rho_k \cdot U_k \cdot F_k \cdot P_k(\cos\vartheta). \tag{1}$$

The quantities are the large-detector correction factor Q_k [15] (see above), the statistical tensor ρ_k, the dealignment factor within the γ-cascade U_k, the angular correlation coefficient F_k and the Legendre polynomials $P_k(\cos\vartheta)$. For the actual transitions the values for the correlation coefficients are listed in the appendix of [9]. Table 2 summarizes the coefficients used in the present calculations. The nuclear alignment A is proportional to the rank 2 statistical tensor ρ_2 and is defined in this paper as

$$A=\frac{3}{I\cdot(2I+1)}\sum_M\left[M^2-\frac{I\cdot(I+1)}{3}\right]\cdot a(M). \tag{2}$$

For an equal population $a(M)$ of the M-substates, $A=0$ is expected, while for a different population $a(M)$ positive alignment up to the value $A=1$ occurs for spin directions in or opposite the beam axis and negative alignment for spin directions perpendicular to the beam axis [9]. The expected signs of the alignment in the fragmentation reaction for different momentum cuts are discussed below. Using the spin values $I=19/2$ and $I=3/2$, the proportionalities $\rho_2=1.924\cdot A$ and $\rho_2=A$ are obtained.

When comparing the small values of the products $U_4\cdot F_4\cdot Q_4$ in Table 2 with the corresponding $U_2\cdot F_2\cdot Q_2$ values, we neglected the $P_4(\cos\vartheta)$ term of the angular correlation.

Hence the values for the angular correlation of the two detectors positioned at an angle of 90° to one another, $W(+45°)$ and $W(-45°)$, were calculated. The normalized function for the $I=19/2$ state, $R=(W(+45°)-W(-45°))/(W(+45°)+W(-45°)\approx -0.48\cdot A$,

Table 2. Coefficients for the angular correlation of transitions in ^{43}Sc

Transition $j_i \rightarrow j_f$	Q_2	U_2	F_2	$U_2 F_2 Q_2$	Q_4	U_4	F_4	$U_4 F_4 Q_4$
19/2→15/2	0.796	1.0000	−0.3717	−0.2959	0.429	1.0000	−0.1577	−0.0677
15/2→11/2	0.865	0.9628	−0.3856	−0.3211	0.602	0.8788	−0.1794	−0.0949
11/2→7/2	0.874	0.9036	−0.4109	−0.3245	0.628	0.7050	−0.2239	−0.0991
3/2→7/2	0.802	1.0000	−0.1429	−0.1146	0.412	1.0000	0	0

was derived. The measured amplitude r of the $R(t)$ functions (Fig. 3) can thus be converted into the measured value of the alignment A. It is about twice the amplitude for the decay of the $I = 19/2^-$ state. A positive spin alignment of ~35% was observed for fragments in the center of the momentum distribution, while the alignment of fragments in the wing of the distribution (Fig. 2) was negative and had a mean value of ~15%. The observed change from a positive alignment to a negative alignment in the wing of the Goldhaber distribution corresponds to the predictions of the model discussed below.

Main features of the projectile fragmentation in peripheral collisions between projectile and target at high energies are well represented by models of an abrasion process followed by deexcitation of the remaining prefragment. In the abrasion step, nucleons are removed from the overlap volume of the projectile whereas the rest of the projectile continues its initial motion. Our major interest in this work is to investigate how well this simple and transparent picture of the reaction applies also to hitherto unexplored observables such as spin alignment and high-spin isomeric ratios.

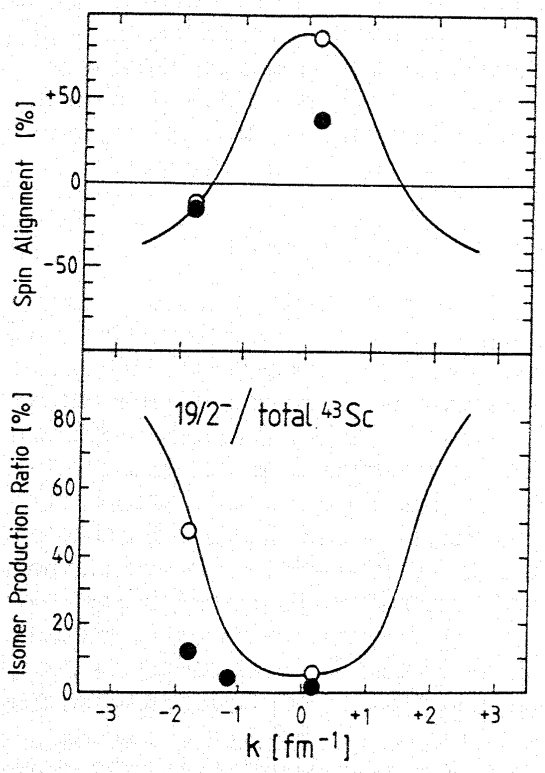

Fig. 4a, b. Comparison of the measured alignment and the isomer production ratio $19/2^-$/total ^{43}Sc as a function of fragment momentum with values from theory [17]. The dots represent the experimental data, the drawn *curves* are the theoretical expectations. The *open circles* are the values calculated from these curves for the actual momentum distributions

For the removal of one nucleon with a position vector $\mathbf{R}_0$ and a Fermi momentum $\mathbf{p}$ from the nuclear surface, the angular momentum transferred to the fragment is $(-\mathbf{p} \times \mathbf{R}_0)$. For the fragments in the wings of the Goldhaber distribution, the directions of the Fermi momenta are in or opposite the beam direction. Thus, the angular momentum of the fragment has a direction perpendicular to the beam axis. This corresponds to a negative alignment [9]. For fragments in the center of the Goldhaber distribution, the spin direction is in or opposite the beam direction and hence a positive alignment is expected. This picture is confirmed in quantitative calculations [17] based on a model of Hüfner and Nemes [4]. We here neglect effects of the deexcitation stage subsequent to the abrasion process and thus assume that the observed alignment of a fragment well represents that for the states populated just after the abrasion process. We take the projectile rest-frame and assume that the projectile has spin 0. According to [4], the cross-section for the abrasion of one nucleon leading to a fragment of a substate j_m with momentum $\mathbf{p}$ is proportional to the probability of finding a particle of substate j_{-m} with $-\mathbf{p}$ at the surface of the target nucleus. The latter probability is given by $W_{j-m}(-\mathbf{p}, \mathbf{R}_0)$ where the distribution function $W_{jm}(\mathbf{p}, \mathbf{r})$ is the Wigner transform of the one-body density matrix $\rho_{jm}(\mathbf{r}', \mathbf{r})$, defined as

$$W_{jm}(\mathbf{p}, \mathbf{r}) = 1/(2\pi)^3 \int \exp(-i\mathbf{p}\cdot\mathbf{s})\, \rho_{jm}(\mathbf{r}+\mathbf{s}/2, \mathbf{r}-\mathbf{s}/2)\, d^3\mathbf{s}. \tag{3}$$

To treat the case of the fragmentation of ^{46}Ti to ^{43}Sc, we extend the above formalism to include a three-body distribution $W_{JM}(\mathbf{p}_1, \mathbf{p}_2, \mathbf{p}_3; \mathbf{r}_1, \mathbf{r}_2, \mathbf{r}_3)$ which is defined similar in terms of the three-body density matrix $\rho_{JM}(\mathbf{r}'_1, \mathbf{r}'_2, \mathbf{r}'_3; \mathbf{r}_1, \mathbf{r}_2, \mathbf{r}_3)$. The subscripts J and M denote the angular momentum and its projection formed by the three nucleons to be removed. Thus, the cross-section for the production of ^{43}Sc fragments of substate JM with momentum p_z is given as

$$\sigma_{JM}(p_z) \propto \int\int dp_x\, dp_y \int dz \iint_{\mathbf{p}_1+\mathbf{p}_2+\mathbf{p}_3=\mathbf{p}} d^3\mathbf{p}_1\, d^3\mathbf{p}_2 \cdot W_{J-M}(-\mathbf{p}_1, -\mathbf{p}_2, -\mathbf{p}_3; \mathbf{R}_0, \mathbf{R}_0, \mathbf{R}_0) \tag{4}$$

where p_z denotes the component of the fragment momentum $\mathbf{p}$ along the z-axis taken parallel to the beam direction, and z the z-component of the position $\mathbf{R}_0(\mathbf{s}, \mathbf{z})$ with $|\mathbf{s}| = R_0$ (nuclear radius). Using σ_{JM}, the alignment for fragments with the momentum p_z is obtained by insert-

ing $a(M)=\sigma_{JM}(p_z)/\Sigma\sigma_{JM}(p_z)$ in (2). The results of the calculated alignment for the $19/2^-$ state using simple shell model wave functions are given in Fig. 4a as a function of the fragment momentum p_z. The mean values of the expected alignment for the actual experimental momentum distributions are compared in Fig. 4a with the experimental values $A\sim 0.35$ for the center, and $A\sim -0.15$ for the wing of the distribution. For the center momentum bin, the observed alignment is only about 50% of the predicted value. In the intermediate momentum cut, contributions from positive and negative alignment unfortunately cancelled each other out. Further experiments should therefore concentrate on the measurement in the very far wings as well as the center of the Goldhaber distribution.

A strong dependence of the isomeric ratio $19/2^-$/total ^{43}Sc from the momentum bin was measured (see Table 1). In Fig. 4b the experimental results are compared with calculated isomeric ratios. These calculations [17] use the coupling of three independent $f_{7/2}$ nucleons to form the $19/2^-$ isomer and the $7/2^-$ ground-state. The predicted increase (Fig. 4b) of the isomeric ratio as a function of decreasing fragment momentum is confirmed in our experiment. The experimental ratios, however, are only about 1/4 of the calculated ones. It should be mentioned that the calculation [17], intended to show the qualitative tendency, does not include one- or two-nucleon abrasion plus evaporation, or the additional abrasion of $d_{3/2}$ nucleons. Such processes reduce the theoretical isomeric ratio, because they contribute to the production of the low-spin states, while the formation of the $19/2^-$ isomer is only realized for the coupling of three $f_{7/2}$ nucleons, one proton and two neutrons, in the substates $m=7/2$, 7/2, and 5/2.

Finally, we would like to point out that in this experiment we implanted the spin-aligned nuclei after slowing them down from relativistic energies. The finding that the alignment is kept in the deceleration process is of large interest for further investigations of nuclear moments of exotic nuclei produced in fragmentation reactions.

References

1. Trautmann, W., Boer, J. de, Dünnweber, W., Graw, G., Kopp, R., Lauterbach, C., Puchta, H., Lynen, U.: Phys. Rev. Lett. **39**, 1062 (1977)
2. Asahi, K., Ishihara, M.: RIKEN Accel. Prog. Rep. **20**, 21 (1986)
3. Asahi, K., Ishihara, M., Ichihara, T., Fukuda, M., Kubo, T., Gono, Y., Mueller, A.C., Anne, R., Bazin, D., Guillemaud-Mueller, D.: Phys. Rev. C**43**, 456 (1991)
4. Hüfner, J., Nemes, M.C.: Phys. Rev. C**23**, 2538 (1981)
5. Schmidt-Ott, W.-D., Asahi, K., Fujita, Y., Geissel, H., Gross, K.-D., Hild, T., Irnich, H., Ishihara, M., Krumbholz, K., Kunze, V., Magel, A., Meissner, F., Muto, K., Nickel, F., Okuno, H., Pfützner, M., Scheidenberger, C., Suzuki, K., Weber, M., Wennemann, C.: GSI Scientific Report 1993, GSI-94-1 (1994)
6. Schwab, T.: PhD Thesis, Darmstadt 1993 (unpublished)
7. Goldhaber, A.S.: Phys. Lett. B**53**, 306 (1974)
8. Geissel, H., Armbruster, P., Behr, K.H., Brünle, A., Burkard, K., Chen, M., Folger, H., Franczak, B., Keller, H., Klepper, O., Langenbeck, B., Nickel, F., Pfeng, E., Pfützner, M., Roeckl, E., Rykaczewski, K., Schall, I., Schardt, D., Scheidenberger, C., Schmidt, K.H., Schröter, A., Schwab, T., Sümmerer, K., Weber, M., Münzenberg, G., Brohm, T., Clerc, H.G., Fauerbach, M., Gaimard, J.-J., Grewe, A., Hanelt, E., Knödler, B., Steiner, M., Voss, B., Weckenmann, J., Ziegler, C., Magel, A., Wollnik, H., Dufour, J.P., Fujita, Y., Vieira, D.J., Sherrill, B.: Nucl. Instrum. Methods B**70**, 286 (1992)
9. Morinaga, H.: Inbeam γ-ray spectroscopy. Amsterdam: North Holland 1976
10. Raghavan, P.: At. Data Nucl. Data Tables **42**, 201 (1989)
11. James, F.: MINUIT reference manual (Version 92.1), Program Library D506. CERN 1992
12. Stöhlker, T.: Private communication 1993
13. Gross, K.-D.: Private communication 1993
14. Slichter, C.P.: Principles of magnetic resonance. Springer Series in Solid-State Scienes. Vol. 1. Berlin, Heidelberg, New York 1978
15. Siegbahn, K.: Alpha-, beta-, and gamma-ray spectroscopy. p. 1691. Amsterdam: North Holland 1965
16. Edmonds, A.R.: Drehimpulse in der Quantenmechanik. Mannheim: BI-Hochschultaschenbücher Bd. 53/53c, 1960
17. Asahi, K., Muto, K.: (to be published 1994)